Genetic variants in *TRPM7* associated with unexplained stillbirth modify ion channel function

James H. Cartwright[1], Qadeer Aziz[1], Stephen C. Harmer[1,2], Sudhin Thayyil[3], Andrew Tinker[1] [#] and Patricia B. Munroe[1] [#]

[1] - Clinical Pharmacology, William Harvey Research Institute, Barts and the London School of Medicine and Dentistry, Queen Mary University of London, Charterhouse Square, London, EC1M 6BQ, UK

[2] – Current address- School of Physiology, Pharmacology and Neuroscience, Faculty of Life Sciences, The University of Bristol, Biomedical Sciences Building, University Walk, Bristol, BS8 1TD.

[3] – Centre for Perinatal Neuroscience, Imperial College London, London W12OHS

*Corresponding Author:

p.b.munroe@qmul.ac.uk & a.tinker@qmul.ac.uk, Tel: 02078825783 Fax: 02078823408, The Centre for Clinical Pharmacology, William Harvey Research Institute, Barts and the London School of Medicine and Dentistry, Queen Mary University of London, Charterhouse Square, London, EC1M 6BQ, UK.

Short title: TRPM7 mutations and stillbirth.

Abstract

Introduction: Stillbirth is the loss of a foetus after 22 weeks of gestation, of which almost half go completely unexplained despite post-mortem. We recently sequenced 35 arrhythmia-associated genes from 70 unexplained stillbirth cases. Our hypothesis was that deleterious mutations in channelopathy genes may have a functional effect *in utero* that may be pro-arrhythmic in the developing foetus. We observed four heterozygous, nonsynonymous variants in *TRPM7*, a ubiquitously expressed ion channel known to regulate cardiac development and repolarisation in mice.

Methods: We used site-directed mutagenesis and single-cell patch-clamp to analyse the functional effect of the four stillbirth mutants on TRPM7 ion channel function in heterologous cells. We also used cardiomyocytes derived from human pluripotent stem cells to model the contribution of TRPM7 to action potential morphology.

Results: Our results show that two *TRPM7* variants, p.G179V and p.T860M lead to a marked reduction in ion channel conductance. This observation was underpinned by a lack of measurable TRPM7 protein expression, which in the case of p.T860M was due to rapid proteasomal degradation. We also report that human hiPSC-derived cardiomyocytes possess measurable TRPM7 currents, however siRNA knockdown did not directly affect action potential morphology.

Conclusion: TRPM7 variants found in the unexplained stillbirth population adversely affect ion channel function and this may precipitate fatal arrhythmia *in utero*.

Introduction

Stillbirth is the devastating loss of a foetus after 22 weeks of gestation during pregnancy. In the UK, there were 4.64 stillbirths per 1000 total births in 2013 (1). The majority of these are caused by obstetric complications, placental insufficiency, genetic disorders, infection and umbilical cord anomalies. However, despite extensive post-mortem investigation, 15-45% of stillbirths go completely unexplained (1-3).

Deleterious mutations within ion channel genes can cause severe arrhythmias and are known causes of sudden death in young adults (4). The cause of death is usually found after a negative post-mortem. We recently sequenced a custom panel of 35 arrhythmia-associated genes in 70 unexplained stillbirth cases from the Cardiac Ion Channelopathies in Stillbirth (CICUS) study (5). We found four cases to have putative pathogenic variants in four long QT syndrome (LQTS) genes, *KCNE1, KCNE2, SCN5A* and *KCNJ2*. We subsequently characterised the functional effect of the heterozygous variant (p.R40Q) found in the *KCNJ2* gene. This gene encodes the inwardly rectifying potassium channel Kir2.1 which controls the resting membrane potential and contributes to cardiac repolarisation (Phase 3)(6). The p.R40Q mutation led to significantly reduced inward currents compared to wild-type channels, which would be predicted to have a deleterious effect on the cardiomyocytes ability to regulate its' membrane voltage. Alongside these data, we observed predicted damaging variants in several other genes, including *TRPM7* a gene implicated from genome wide association studies of QT interval (7). Four heterozygous nonsynonymous variants were observed in *TRPM7* in four individual cases.

Transient receptor potential melastatin 7 (TRPM7) is a non-selective cation channel with a serine/threonine kinase domain in the C-terminus and is ubiquitously expressed in mammalian cells (8). Current opinion regards TRPM7 as a key transporter of divalent cations (Zn^{2+}, Mg^{2+} and Ca^{2+}) across the cell membrane (9, 10); while the α-kinase is capable of phosphorylating downstream effector kinases and modifying chromatin (11, 12).

TRPM7 plays a key role in dictating cell proliferation, survival, apoptosis alongside organogenesis and embryonic survival (13-16). A previously reported genetic variant, p.T1482I, has been shown to increase the sensitivity of TRPM7 to inhibition by Mg^{2+} (17). Temporal control of *TRPM7* expression in the mouse embryo is required for correct cardiac development (15).

The four nonsynonymous variants in *TRPM7* lie within conserved amino acid positions and were predicted to functionally affect the protein by at least one of three predicted software tools (PolyPhen, SIFT or Mutation Taster (18, 19)). The first two, p.G179V and p.R494Q lie within the N-terminal domain of TRPM7. The third, p.T860M is within the second transmembrane domain, whilst the final variant, p.E1205G resides in the C-terminal domain, upstream of the alpha kinase (Table 1).

In this study we transfect a TRPM7 expressing plasmid into HEK293 and CHO-K1 cells and record the resulting current using whole-cell patch-clamp electrophysiology. We demonstrate that three TRPM7 variants (p.G179V, p.R494Q and p.T860M) significantly alter current densities in comparison to the wild-type ion channel. This effect was not due to an altered response to magnesium inhibition, nor was *TRPM7* transcription perturbed. Instead, we found a lack of protein expression in p.G179V and p.T860M transfected cells, alongside an increase in p.R494Q protein. Interestingly, inhibiting the 26S proteasome with MG132 treatment increased p.R494Q expression and inhibited p.T860M expression. To further characterise the importance of *TRPM7* in developing cardiac myocytes, we measured TRPM7 current in hiPSC-derived cardiomyocytes. While we found TRPM7 expression to increase in the early stages of differentiation, and there is a large outward TRPM7-like current, knockdown with TRPM7 siRNA had no effect on cardiomyocyte action potential morphology.

Results

Expressing TRPM7 in HEK293 and CHO-K1 cells

To ascertain the effect the nonsynonymous mutations may have on TRPM7 function we transfected both CHO-K1 and HEK293 cells with a wild-type TRPM7 expression plasmid. After 5-10 minutes of dialysis, large outward currents were detected, with an I-V relationship typical of TRPM7 (Figure 1A). We analysed outward and inward current at +80mV and -80mV respectively, in both CHO-K1 and HEK293 cells (Figure 1B-C). Using CHO-K1 cells, we demonstrated these currents were susceptible to inhibition to 10mM magnesium (Figure 1D-F). Current density was also susceptible to inhibition by treatment with 50μM 2-APB (Figure 1G-H). HEK293 cell TRPM7 current was also inhibited by treatment with extracellular magnesium (data not shown). These data confirmed we had an efficient expression system to test the effect of our stillbirth sequenced variants on TRPM7 function.

Variants alter TRPM7 current density in CHO-K1 and HEK293 cells

We transfected both cell lines with the four variants of TRPM7 and recorded the current-voltage relationships. Due to its likely endogenous expression in both cell lines, we found TRPM7 I-V relationships in all cells (Figure 2). However when analysing grouped current density data we found a significant reduction in current density in CHO-K1 cells when transfected with p.G179V ($P < 0.05$, Figure 2A). We also saw a significant increase in current density at both +80mV and -80mV when expressing p.R494Q compared to wild-type transfected cells ($P < 0.001$, Figure 2A). When these experiments were repeated in HEK293 cells, we found that both p.G179V and p.T860M current density was markedly reduced compared to wild-type TRPM7 ($P < 0.01$ respectively) with a trend to reduction for E1205G (Figure 2B). However, in comparison to CHO-K1 expression of p.R494Q, current density was equal between wild-type and p.R494Q expressing cells ($P = 0.98$, Figure 2B).

Reducing extracellular Mg^{2+} amplifies difference between wildtype and mutant TRPM7 channels

We wanted to investigate whether the stillbirth mutations were affecting the TRPM7 channels response to magnesium inhibition. We perfused transfected CHO-K1 cells with extracellular solution supplemented with increasing concentrations of magnesium from 0.5mM to 6mM after allowing current recordings to plateau. In these experiments, we found a significant decrease in current density at +80mV in cells transfected with either p.G179V or p.T860M TRPM7 compared to wild-type channels, but only at 0mM Mg^{2+} ($P < 0.01$ and 0.05, respectively, Figure 3A & C). However, when bath magnesium was increased any difference in Mg^{2+}-dependent inhibition between these variants and wild-type TRPM7 was attenuated and eventually abolished. Cells expressing p.R494Q TRPM7 showed a significant increase in current density at +80mV compared to wild-type cells at both 0mM and 0.5mM Mg^{2+} ($P < 0.001$, Figure 3B). We calculated the IC_{50} for WT transfected cells at 0.62mM Mg^{2+} with a Hill coefficient of -1.21. Further analysis of stillbirth variant transfected cell IC_{50} and Hill coefficient values were not significantly different to WT TRPM7 (Supplementary Table 3). Interestingly, the inward current for this variant analysed at -80mV was increased compared to wild-type TRPM7 at 0mM, 0.5mM and 1mM Mg^{2+} ($P < 0.001$, 0.001 and 0.05, respectively, Figure 3E). Suggesting that despite physiological levels of magnesium this variant increased both inward and outward ionic conductance compared to the wild-type TRPM7 channel. These data also suggest that any difference in whole-cell TRPM7 ion channel conductance are not the result of a variants influencing the channels response to magnesium inhibition, but are more likely due to alterations in expression.

In summary, our electrophysiological data show that G179V and T860M result in a loss of channel function and R494Q a gain of function which was particularly apparent in conditions of low extracellular Mg^{2+}.

Effect of variants on TRPM7 protein and mRNA expression in heterologous cells

To investigate whether this decrease in current density was due to altered protein levels, whole cell lysates were harvested from transfected cells and western blotting was performed. p.G179V and p.T860M TRPM7 mutants did not express well in transiently

transfected cells (Figure 4A). Densitometry measurements showed a significant decrease in HEK293 cells transfected with either p.G179V or p.T860M TRPM7 compared to WT TRPM7. However, when we investigated TRPM7 and mutant mRNA levels in these cells using qPCR, the mRNA expression level was similar (Figure 4C). To test whether this reduction in protein was due to rapid degradation, we harvested cell lysates after overnight treatment with the proteosomal inhibitor MG132. We observed an increase in p.R494Q transfected cells compared to wild-type, and we may have able to detect low level expression of p.T860M TRPM7 protein (Supplementary Figure 1).

Confirming the presence of TRPM7 current in hiPSC-derived cardiomyocytes

We used an *in vitro* model of cardiomyocyte generation using hiPSC cells to first ascertain TRPM7 expression in human cardiac cells, and to test the effect that reduced TRPM7 expression may have on the electrophysiological properties of cardiomyocytes. We used an in-house hiPSC line (named HS1M) and differentiated the cells into cardiomyocytes using a previously published protocol (Supplementary Figure 2)(20). hiPSCs initially expressed high levels of TRA-1-60 and three key pluripotency markers which rapidly decreased by 7 days of differentiation (20). Individual cells stained positively for cardiac troponin T (Figure 5A). We observed variation in *TRPM7* expression during differentiation, with cardiomyocytes at day 21 expressing more than double that observed in hiPSC cells, but this was not significant (Figure 5B). In contrast, pluripotency markers rapidly decreased as the cell differentiated (Supplementary Figure 2C).

Beating hiPSC-CMs were seeded onto gelatin coated class coverslips at low density at days 15-16 for single-cell patch-clamp analysis to detect TRPM7 current at days 21-23. We found in all contractile cells subjected to whole-cell patch-clamp, typical TRPM7 currents which were detected after dialysis of cells with Mg^{2+} chelating intracellular solutions. Although initial break-in currents were minimal, outward currents at +80mV were detected after 5-10 minutes (Figure 5C, E & F). We perfused the bath solution with magnesium to confirm these currents were generated by TRPM7 (Figure 5D-F). We found that at both

+80mV and -80mV, these currents were susceptible to magnesium inhibition ($P < 0.001$) which could be reversed following washout with standard extracellular solution.

Mimicking TRPM7 reduction using siRNA does not adversely affect action potential parameters in hiPSC-derived cardiomyocytes

To mimic possible haploinsufficiency of TRPM7 in developing cardiac cells due to p.G179V and p.T860M mutants, we used siRNA to reduce mRNA levels. To patch-clamp cells that had taken up TRPM7 siRNA we co-transfected siGLO. Whole-cell patch clamp analysis showed markedly reduced outward currents at +80mV ($P < 0.001$, Figure 6A-B) in cells transfected with TRPM7 siRNA. On average this led to a 25.5 pA/pF reduction in current density, a similar reduction to that seen in 10mM Mg^{2+} treated cells (28.1 pA/pF). Perhaps due to their small initial size (<5pA/pF), inward currents at -80mV were not significantly different between control cells, those perfused with 10mM Mg^{2+} or those transfected with TRPM7 siRNA (Figure 6C). RT-qPCR analysis of these cells found a significant decrease in TRPM7 mRNA levels in siRNA transfected populations (Supplementary Figure 3). After confirming TRPM7 knockdown, we recorded triggered action potentials in a separate set of experiments (Figure 6D-E). To establish whether there were any deleterious electrophysiological effects caused by reducing TRPM7 ion channel expression we analysed action potential morphology. (Figure 6G-L). We found that there were no statistical differences in action potential duration, minimum diastolic potential, resting membrane potential and peak voltage amplitude in the action potentials of cells transfected with scrambled or TRPM7 targeted siRNA and untransfected cardiomyocytes.

Discussion

Almost half of stillbirths go unexplained, despite extensive post-mortem analysis. In this study we present data from previously sequenced and predicted damaging *TRPM7* genetic variants found in unexplained stillbirth cases (5). There is extensive research studying ion channelopathies that cause sudden cardiac death in young adults, however there is little evidence of harmful ion channel variants in stillbirth (21). TRPM7 is required for mammalian cardiac development, and genetic variation within the gene has been linked to a prolonged QT interval (7, 15). To investigate the role these variants may play in perturbing the function of the TRPM7 ion channel, we used heterologous expression and hiPSC-CMs to study channel function, magnesium response, and expression.

Here we show that three *TRPM7* variants modify ion channel function in comparison to the wild-type channel and identify TRPM7 as an ion channel present in hiPSC-derived cardiomyocytes. First, we expressed and characterised the wild-type channel in HEK293 and CHO-K1 cells before analysing the effects of the four TRPM7 mutants. We report that p.G179V and p.T860M variants reduced outward currents significantly compared to the wild-type channel. Conversely, in a CHO-K1 specific manner, p.R494Q increased observed current density at both +80mV and -80mV. This increase remained significantly different despite inhibition with 1mM Mg^{2+}.

Protein expression data confirmed that decreased current density caused by the p.G179V and p.T860M variants was due to reduction in protein expression. In the case of p.T860M this was at least in part due to rapid proteosomal degradation. It has been shown that TRPM7 is required for proper embryonic development and cardiogenesis in mice (15, 16). Targeted cre-mediated knockdown of TRPM7 before E10 leads to congestive heart failure due to lack of myocardial compaction. Later deletion at E12.5 of gestation can lead to cardiomyopathy, heart block and impaired repolarisation. Given the experimental data it is feasible to postulate that a reduction in TRPM7 function/expression during gestation could

have an adverse effect on human cardiac development. Mechanistically it is hard to determine the mechanisms that underlie this effect as TRPM7's role in magnesium and zinc homeostasis, alongside control of apoptosis and gene expression is still under investigation (10, 12, 13, 22). Reduced TRPM7 expression may limit the cell's ability to take-up divalent cations or hinder their expulsion – alongside adverse changes to a cell's gene expression profile.

Recent work with cryo-EM microscopy has revealed the closed state structure of mouse TRPM7 at the Ångstrom scale (23). These data show several interactions between the N-terminal domain and the inner plasma membrane, TRP domain or C-terminal domain. Non-synonymous variants found within these structural motifs may destabilize the protein, resulting in misfolding and degradation.

Using a hiPSC-derived model, we demonstrate that TRPM7 can be found in immature human cardiomyocytes 21 days-post differentiation. Analysis of temporal *TRPM7* expression during cardiomyocyte differentiation showed a gradual increase in mRNA, alongside the reduction in pluripotency factors. Single-cell patch-clamp revealed that these cells possess relatively large quantities of TRPM7 present at the plasma membrane, with mean outward currents of (~33.3 pA/pF). Both treatment with Mg^{2+} and siRNA transfection significantly reduced these currents, strongly suggesting their identity as TRPM7. There is evidence to suggest that TRPM7 can regulate cardiomyocyte ion channel gene expression, alongside acting as a cation channel in its own right (12, 15, 16). However, when we mimicked possible TRPM7 haploinsufficiency we could not detect an effect on action potential morphology. This may be due to the temporal aspect indicative of the TRPM7 knockout phenotype, shown in mice to vary from lethal to mildly perturbed repolarisation depending upon the gestational stage at which TRPM7 is removed. A more severe effect may occur if siRNA to TRPM7 was transfected during differentiation, and this an area which warrants further *in vitro* experimentation to identify critical windows of TRPM7 expression during hiPSC-derived cardiomyocyte maturation. It is notable that increases in TRPM7 expression

occur relatively early in hiPSC cardiac differentiation. It is an open issue whether TRPM7 currents contribute significantly to the foetal cardiac action potential. Our experiments with siRNA suggest that this isn't the case under physiological ionic conditions, particularly due to the inhibitory effect of intracellular Mg^{2+} present in the tissue. Alternatively, haploinsufficiency may have deleterious effects that are not solely related to effects on cardiac excitability but to effects on cell survival mediated by the kinase domain.

In summary, we found two variants in *TRPM7*, p.G179V and p.T860M reduce ion channel current expression, which in the case of p.T860M is likely due to rapid degradation mediated by the proteosome. In addition, the p.R494Q TRPM7 variant significantly increases TRPM7 ion channel current, in a cell-type specific manner. For the first time we report that a TRPM7 current is present in hiPSC-CMs. However, siRNA inhibition at day 15-16, despite reducing TRPM7 current, did not alter AP duration. We believe that *TRPM7* may play a key role in ensuring correct cardiac development of the foetus. TRPM7 is the major Ca^{2+} channel in atrial fibroblasts, and upregulation of these transients is reported in patients with atrial fibrillation (24)(24). Significant increases in these Ca^{2+} influxes from p.R494Q TRPM7 in the developing atrial myocardium could predispose developing foetal hearts to atrial fibrillation. In a similar fashion a reduction in TRPM7 current may also predispose to cardiac arrhythmia. For example it is known that both long and short QT syndromes arising from loss and gain of function mutations respectively in KCNQ1 can result in sudden cardiac death in afflicted families (25)(25). Therefore, any changes to TRPM7 abundance during early cardiogenesis may have severe downstream effects later in gestation, potentially creating a pro-arrhythmic cardiac environment. Linking causation with genetic variation is inherently difficult but functional assays of potential impairment of protein function can contribute significantly to assessing potential pathogenicity (26). Our data indicate inherited or *de novo TRPM7* mutations may increase the risk of unexplained stillbirth and this warrants further attention.

Materials and Methods

Cell culture, plasmids and transfection

Human Embryonic Kidney-293 cells (HEK293) were a gift from Professor Lily Jan (Howard Hughes Medical Institute, San Francisco, USA). Chinese Hamster Ovary-K1 (CHO-K1) cells were obtained from the European Collection of Authenticated Cell Cultures (supplied by Sigma – 85051005)). HEK293 and CHO-K1 cells were cultured in minimum essential medium (31095029, Gibco, ThermoFisher) and Ham's F12 medium (N6658, Sigma-Aldrich), respectively. Both media were supplemented with 10% FBS (10500056, Gibco, ThermoFisher) and 100 units/mL of penicillin and 100 µg/mL of streptomycin (15140122, Gibco, ThermoFisher).

A pcDNA4/TO plasmid containing the *TRPM7* gene (RefSeq NG_021363.2, NM_017672.6), and a tetracycline repressor plasmid, pcDNA6/Tet Repressor were both kind gifts from Professor Schmitz (11). An eGFP plasmid (Clontech) was used to identify successfully transfected cells. Transfection was carried out using: FuGENE® HD (E2311, Promega) or NovaCHOice ® (72622-3, Merck) as per manufacturer's instructions. Briefly, reactions of TRPM7 vector and Tet Repressor plasmid were mixed with the transfection reagent in 37˚C Opti-MEM® reduced serum media. After 5-6 hours, transfection complexes were removed and fresh media added. Precisely 24 hours later, growth media was changed, this time supplemented with 1µg/mL of tetracycline (87128, Sigma-Aldrich). Cells were harvested/analysed 24-48 hours after tetracycline induction.

Patch-clamp electrophysiology

Whole-cell patch-clamp recordings were made at room temperature (21-25˚C), using a multiclamp 700B and digitised using a Digidata 1550B (Molecular Devices). The internal pipette contained (in mM): 145-Cs-methanesulfonate ($CsSO_3CH_3$), 8 NaCl, 10 HEPES and 10 EGTA; pH 7.2 with CsOH. The extracellular solution contained (in mM): 145 NaCl, 5 KCl, 2 $CaCl_2$, 10 Glucose and 10 HEPES (pH 7.4 with NaOH). For measuring TRPM7 current in

hiPSC-CMs, the internal pipette solution contained (in mM): 120 L-aspartic acid, 20 CsCl, 2.5 EGTA, 2.5 EDTA, 10 HEPES, 120 CsOH, 5 Na_2GTP (pH 7.2 with CsOH). Extracellular solution contained (in mM): 135 NaCl, 5.4 CsCl, 10 HEPES, 10 Glucose, 0.1 $CdCl_2$ and 1$CaCl_2$ (pH 7.4 with NaOH). To record action potentials, internal pipette solution contained (in mM): 110 K-Gluconate, 20 KCl, 10 HEPES, 0.05 EGTA, 0.5 $MgCl_2$, 5 Mg ATP, 0.3 Na_2-GTP and 5 Na_2 phosphocreatine (pH 7.4 with KOH). Extracellular solution for action potential recordings (mM): 140 NaCL, 2.7 KCl, 1 $MgCl_2$, 2 $CaCl_2$, 0.5 Na_2HPO_4 and 5 glucose (pH 7.4 with NaOH). Only cells with membrane resistance >800MΩ and access resistance <10MΩ were used in analysis.

Pipettes were backfilled with intracellular solution to resistance 2 – 3 MΩ. Pipette tips were coated with SigmaCote to reduce pipette capacitance (SL2, Sigma-Aldrich). Series resistance was set to 70% compensation using the in-built amplifier circuitry. After whole-cell configuration was established, recording began immediately to observe current run-up. We used a ramp voltage protocol to measure TRPM7 current: the holding potential was set at 0mV before lowering to -100 mV and then raised to +100 mV over 250 ms before returning to 0mV. For time-course analysis experiments this was measured every 5 seconds from electrical access being established through the cell. Data was analysed using Clampfit 10.5 (Molecular Devices).

In hiPSC derived cardiomyocytes (hiPSC-CMs), we only analysed triggered action potentials (APs) from cells which spontaneous action potentials. APs we triggered using a current pulse (between 400-800pA) at a frequency of 1Hz. To calculate action potential duration, the time (in ms) was calculated as the time it took for membrane potential to return to 50% and 90% (APD_{50} and APD_{90}) of the resting membrane potential after current trigger. Cells were paced for 50 seconds before recording the final 10 action potentials. These results of the final 10 traces were combined to give an ‘average’ action potential for every cell. We did not analyse cells according to ventricular-like or atrial-like categorisations due to a limited number of cells.

Protein Harvesting, SDS-PAGE and Western Blotting

HEK293 cells were transfected at ~70% confluence as previously mentioned and harvested 24 hours after tetracycline induction. Cells were washed with PBS^+ (0.1mM $CaCl_2$ and 1mM $MgCl_2$) before a 30-minute incubation on ice with NP-40 lysis buffer containing protease inhibitors (11816170001, Sigma-Aldrich). Lysates were scraped into pre-chilled tubes and cleared by centrifugation at 10,000 *g* for 10 minutes at 4˚C. 20µg of protein was loaded for each well into 6% polyacrylamide gels. Resolved proteins were transferred to PVDF membranes overnight and then blocked for one hour in PBS-T with 5% milk powder or 1% BSA (A2153, Sigma-Aldrich). Membranes were then incubated with either anti-TRPM7 (sc-271099, Santa Cruz) or β-actin (ab8226, Abcam) antibodies for one hour at room temperature. Secondary antibodies were incubated for one hour at room temperature before imaging with Amersham ECL western blotting detection reagent (GE Healthcare). Primary and secondary antibody details are listed in supplementary table 1. ImageJ software was used to quantify TRPM7 expression which was normalised to loading control β-actin levels, and then all stillbirth variant expression was normalised to the WT value in the same gel. For proteosomal inhibition experiments, cells were treated with 5µM MG132 (Sigma-Aldrich) for 16 hours prior to harvesting.

RNA Harvesting and Quantitative PCR

Total cell RNA was harvested using a RNeasy mini kit (Qiagen) as per manufacturer's instructions either 24h after tetracycline induction or at specific time points of stem cell differentiation. During harvesting of RNA, the column was treated with DNase I for 15 minutes at room temperature. RNA was diluted in nuclease free water, and 50ng used per qPCR reaction. All probes used are listed in Supplementary Table 2. Data was analysed using $2^{-\Delta\Delta Ct}$ method normalised to loading control and then normalised to wild-type. To calculate gene expression in hiPSC-derived cardiomyocytes, RNA levels were first normalised to the housekeeping gene GAPDH. All expression values were then normalised to the expression of the gene of interest in naïve iPSC cells prior to differentiation.

Confocal Microscopy

Cells were first washed with PBS^{+} to remove media and then fixed with 3.7% formaldehyde (Sigma-Aldrich) for 10 minutes at room temperature. Cells were permeabilised with PBS Triton X-100 0.1% for 10 minutes. We blocked cells in PBS-T 5% milk for one hour and carried out primary anti cTnT incubation for overnight at 4˚C. Fluorescent secondary antibody incubation took one hour at room temperature. All antibody details are listed in supplementary table 1. Nuclei were counter stained with DAPI and all slides stored at 4˚C until imaging with an LSM710 confocal microscope (Zeiss).

Human Stem Cell-Derived Cardiomyocytes

Healthy human induced pluripotent stem cell line (named - HS1M) were generated and maintained as previously described (27). Cardiomyocytes were differentiated using a protocol based upon previous work published by Burridge et al (20). In brief, hiPSCs were seeded at 150,000 cells/cm^2 in a 24-well plate and allowed to reach ~80% confluence over 48 hours. Media was changed to 'CDM3' (RPMI1640 (Thermofisher) supplemented with 500µg/ml *O.sativa*-derived recombinant human albumin (Sigma-Aldrich), 213µg/ml L-ascorbic acid 2-phosphate (Sigma-Aldrich)) with 6µM CHIR99021 (Sigma-Aldrich). After 48 hours, media was changed to CDM3 supplemented with 2µM C59 for a further two days before regular CDM3 media changes every 2-3 days. For patch-clamp analysis, at 15 days post differentiation, cells were treated with TrypLE Express (Thermofisher) for 10 minutes at 37˚C and seeded onto glass coverslips at a density of 10,000 cells/cm^2.

For TRPM7 siRNA knockdown experiments, 48 hours before patch-clamp analysis, adhered cells were transfected with either SMARTpool: ON-TARGETplus TRPM7 targeting siRNA or a scrambled control (L-005393-00-0005 or L-006233-00-0005 respectively, Dharmacon). DharmaFECT transfection reagent 1, 2.5µL/well (T-2001-02, Dharmacon) was used to transfect 2.5µL/well of 2µM siRNA.

Statistics

All data was analysed with GraphPad Prism 6. Grouped data were tested with one-way ANOVA, using Dunnett's multiple comparison to test variants vs wild-type unless otherwise stated. For individual analysis of two groups, unpaired t-tests were used to calculate statistical differences. When comparing two independent variables, two-way ANOVA with Sidak's multiple comparison test was used. All group data is presented as mean ± S.E.M. Significant P values are denoted as * = $P < 0.05$, ** = $P < 0.01$ and *** = $P < 0.001$.

Acknowledgments

This work was funded by the British Heart Foundation (BHF), as part of the 4 year PhD scheme at QMUL grant number FS/13/58/30648 and programme grant RG/15/15/31742 and by Stillbirth and Neonatal Death Society (SANDS) in collaboration with Wellbeing of Women from funding provided by SANDS (grant Number RG1248). This work forms part of the research program of the National Institutes of Health Research (NIHR) Cardiovascular Biomedical Centre at Barts and The London, Queen Mary University of London. SCH was supported by a BHF Intermediate Basic Science Research Fellowship [FS/12/5/29756].

Conflict of Interests

The authors declare no conflict of interests.

Table 1

Mutation	Domain	GERP++	PolyPhen	Mutation Taster	SIFT	gnomAD Frequency
c.G536T p.G179V	N-terminal	4.65	1	1	0	7.48e-5
c.G1481A p.R494Q	N-terminal	4.11	1	1	0.21	1.71e-5
c.C2579T p.T860M	Transmembrane	5.59	1	1	0	7.44e-6
c.A3614G p.E1205G	C-terminal	5.3	0.561	1	0	1.90e-5

Table 1. Summary of TRPM7 variants found in stillbirth cases. We sequenced four predicted damaging variants represented as both cDNA (c.) and protein (p.) changes. Listed are their relative locations within known domains of the TRPM7 protein. GERP++ score estimates the level of functional constraint that DNA position is under, within coding regions the average score is conservation score is 2 (28). Polyphen and SIFT scores rate amino acid substitutions on their probability of impacting protein structure and function by providing values between 0 and 1 (18, 19). Variants rated above 0.85 by Polyphen are confidently predicted to be damaging, while those rated below 0.05 by SIFT are considered likely to be deleterious. Mutation taster analyses substitutions based upon base conservation, specific amino acid substitutions, functional domain location and other possible splicing effects. All TRPM7 variants were rated as 1 and annotated as disease causing. gnomAD frequency represents the variant's abundance in the online genome aggregation database project, containing 125,748 exome sequences.

Figure 1. **TRPM7 current recorded from transfected CHO-K1 and HEK293 cells. A** Representative TRPM7 current trace from CHO-K1 cell transfected with TRPM7 at initial break-in (t=0s) and after current run-up (t=500s). **B** Current density at +80mV from both CHO-K1 and HEK293 cells transiently transfected with TRPM7 (red) compared with untransfected cells (black). **C** Matching inward current density from cells in A, analysed at -80mV. **D** Whole-cell current trace before (black) and after (red) addition of 10mM magnesium to extracellular solution during whole-cell recording of a WT TRPM7 transfected CHO-K1 cell. **E** Time course of CHO-K1 whole-cell current showing immediate inhibition following 10mM magnesium treatment. **F** Summary of whole-cell peak current data and following 10mM magnesium treatment in both WT TRPM7 transfected and UT CHO-K1 cells at +80mV. **G** Whole-cell current trace before (black) and after (red) addition of 50µM 2-APB to extracellular solution during whole-cell recording of a WT TRPM7 transfected CHO-K1 cell.. **H** Time course of current at +80mV from cell shown in (G), showing current reduction over 300seconds following 2-APB addition. **H** WT = wild-type, UT = untransected. * - P<0.05, *** - P<0.001.

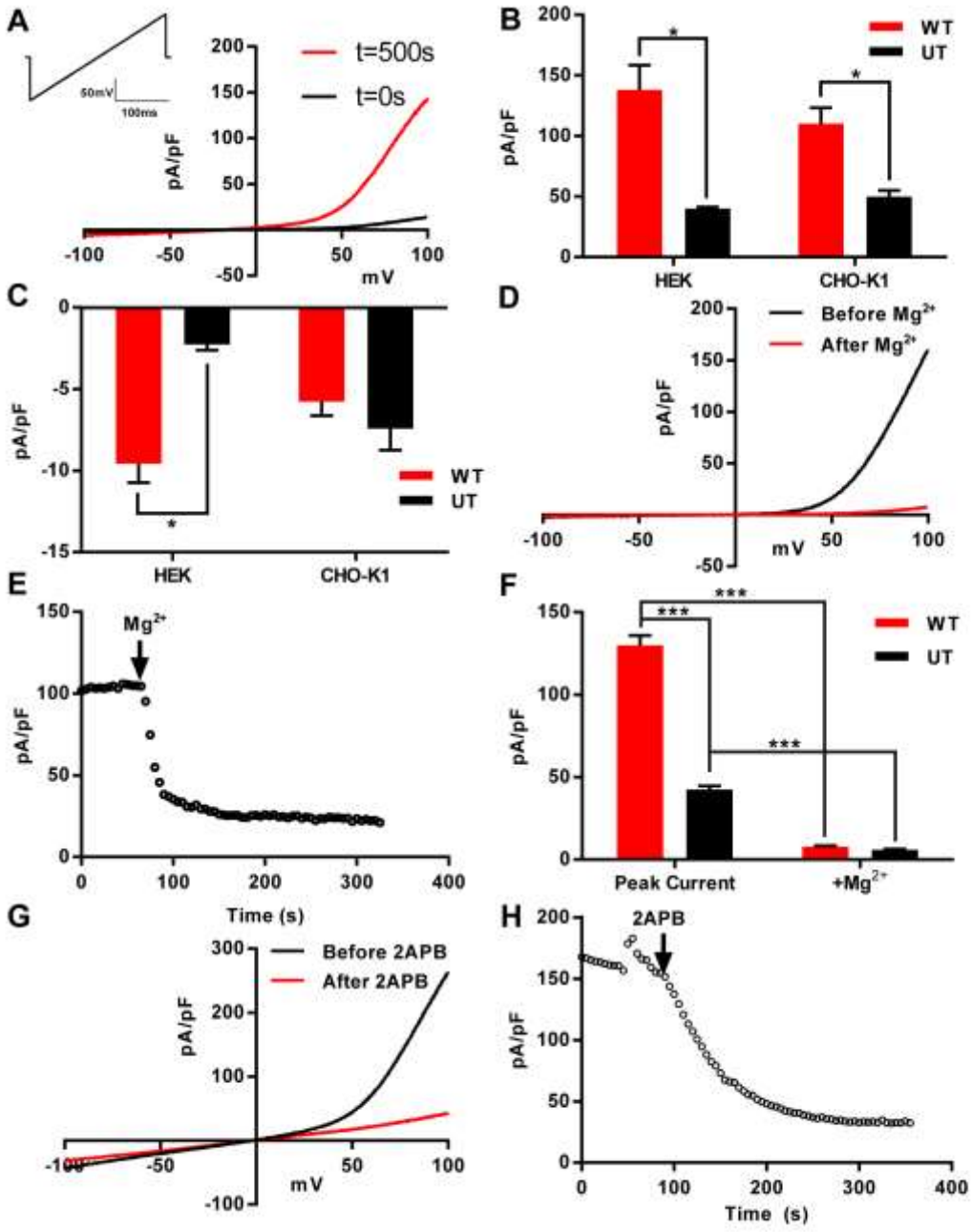

Figure 2. **Stillbirth TRPM7 variants alter current density in a cell-specific manner. A** Summary data of average TRPM7 current density at +80mV (red) and -80mV (blue) from CHO-K1 cells (WT n = 28, variant n = 13-8). **B** Summary data of average TRPM7 current density at +80mV (red) and -80mV (blue) from CHO-K1 cells (WT n = 24, variant n = 12-7) **C** Whole-cell current trace recordings from CHO-K1 cells transiently transfected with WT, p.G179V, p.R494Q, p.T860M and p.E1205G TRPM7. WT = wild-type. * - P<0.05, ** - P <0.01, *** - P<0.001.

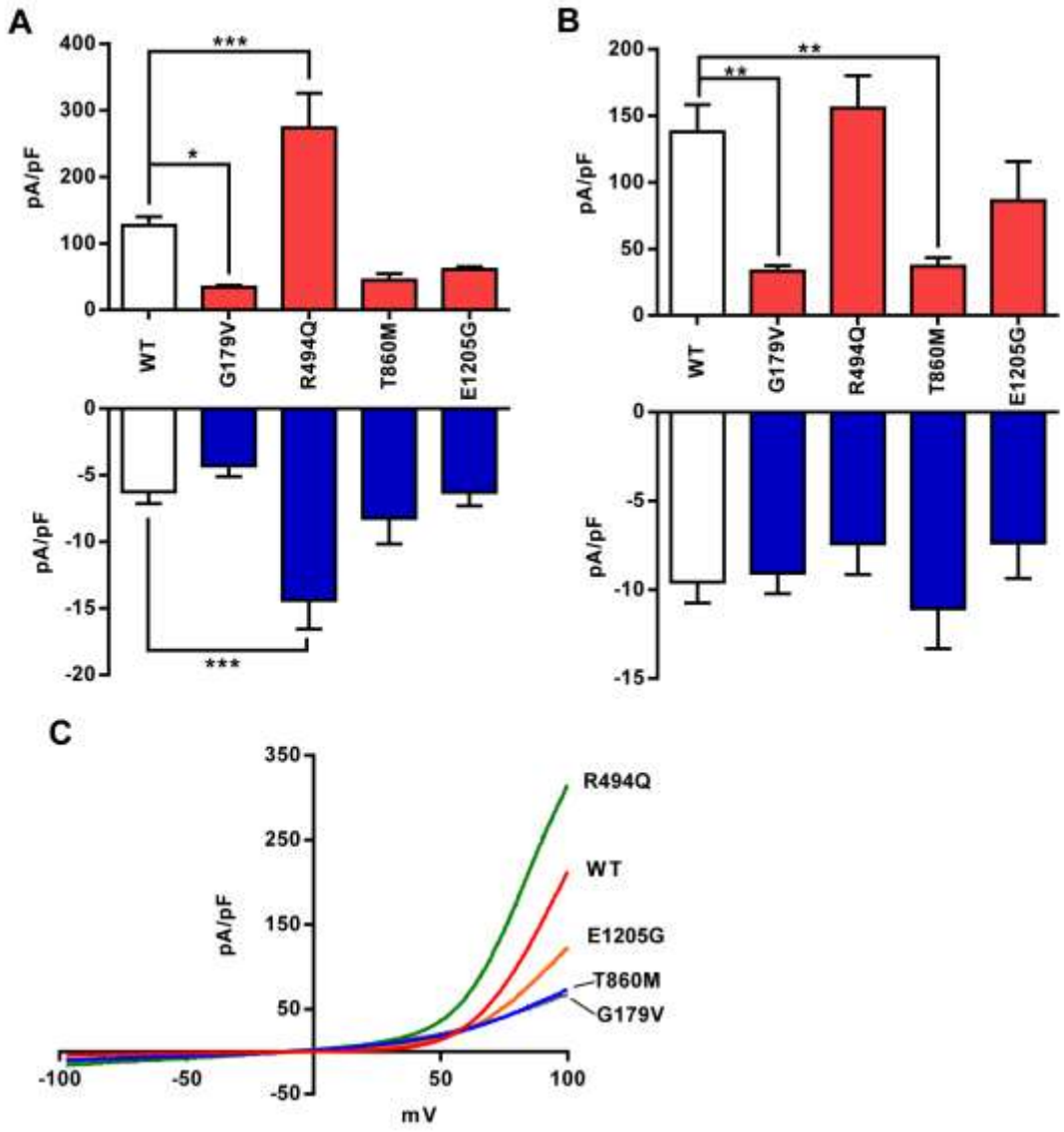

Figure 3. **Stillbirth variants alter TRPM7 current density at low concentrations of magnesium. A-D** Average TRPM7 current density recorded from transfected CHO-K1 cells at +80mV in response to increasing concentrations of bath magnesium (n = 7-8). **E** Average inward current density (-80mV) of cells transfected with p.R494Q TRPM7 **F** Voltage protocol used throughout these experiments. Holding potential was set at 0mV and the protocol repeated every 5 seconds. WT = wild-type, UT = untransfected. * = P<0.05, ** = P<0.01, *** = P<0.001 vs WT.

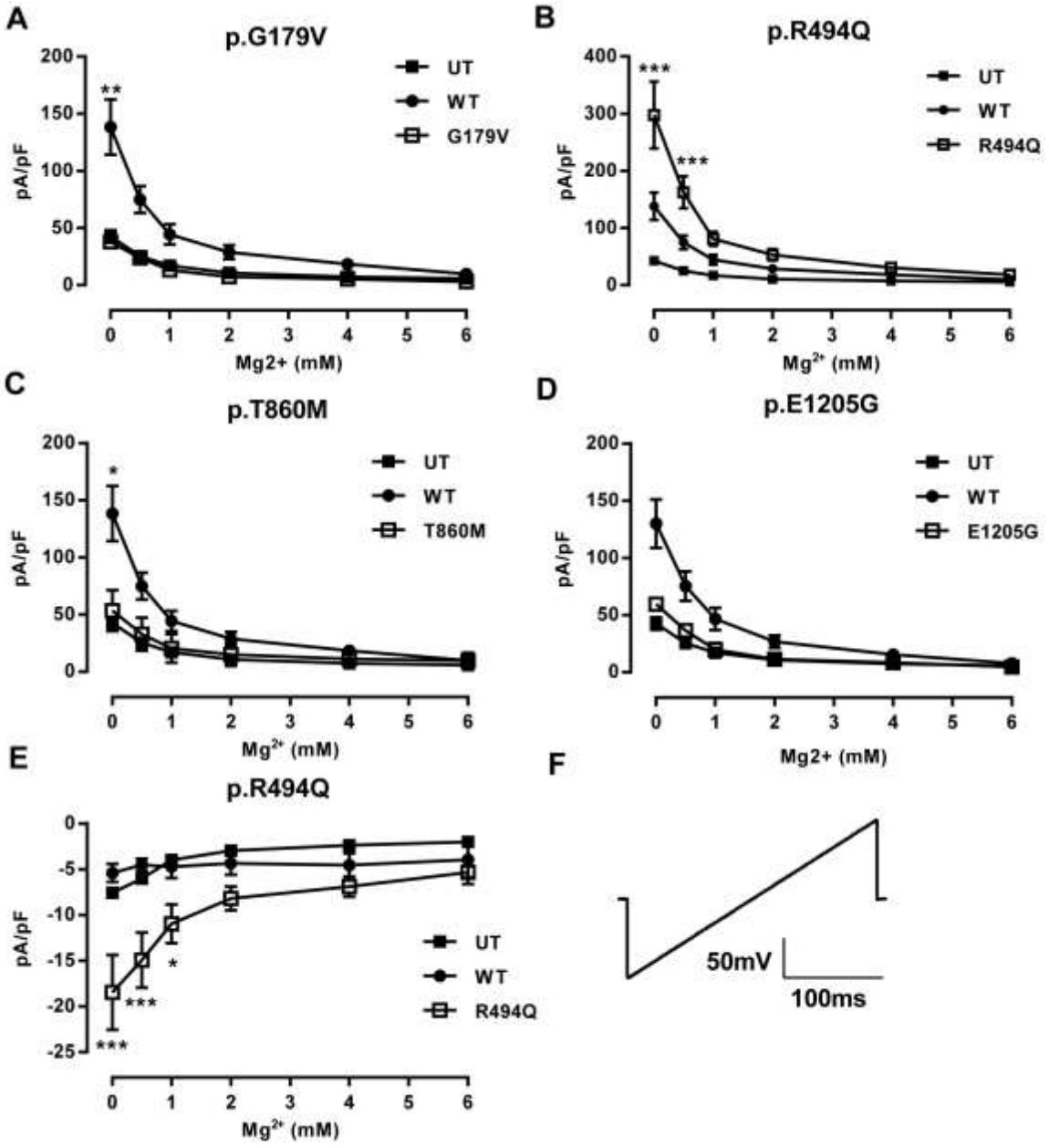

Figure 4 **Stillbirth variants p.G179V and p.T860M reduce TRPM7 protein levels but leave transcription unchanged. A** Whole cell lysates from HEK293 cells transiently transfected with wild-type TRPM7 and mutant vectors. PVDF membranes were initially blotted with anti-TRPM7 before stripping and reprobing with anti-β-actin. **B** Quantification of three western blots from whole-cell HEK293 lysates transfected with WT or stillbirth variant TRPM7 normalised to loading β expression before normalising to WT expression. **C** qPCR expression of TRPM7 from transfected cell lysates normalized to WT. Lysates were treated with DNase I for 15 minutes at room temperature before qPCR analysis. **D** Whole cell lysates from HEK293 cells treated overnight with 5μM MG132. Cells were transfected with wild-type and mutant TRPM7 vectors before overnight incubation with proteosomal inhibitor. WT = wild-type, UT = untransfected. *** = P<0.001 vs WT.

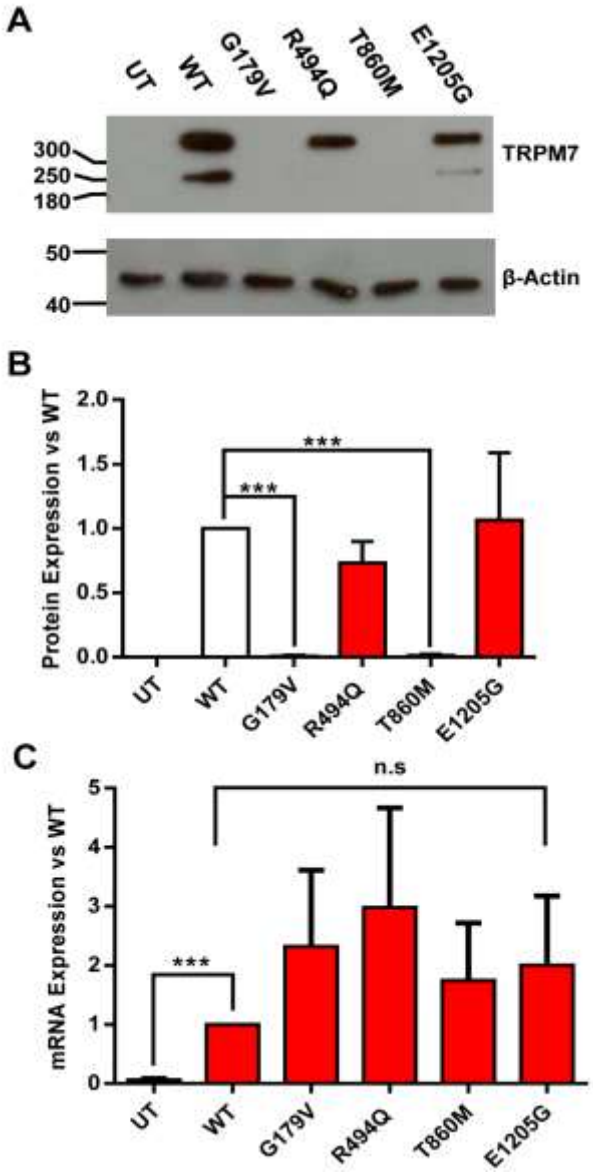

Figure 5 **A TRPM7-like current can be found in 21 day old hiPSC-derived cardiomyocytes. A** Staining of hiPSC-CMs after 21 days of differentiation for cardiac troponin (cTnT) and DAPI. **B** qPCR analysis of TRPM7 expression levels over the course of hiPSC-CM differentiation. TRPM7 expression at each timpoint was normalized to GAPDH expression before being compared to TRPM7 expression in undifferentiated hiPSC cells. **C** A representative TRPM7 trace from whole-cell hiPSC-CMs. Initial current is shown (black) at initial current recordings before magnesium is removed from the bath, and a steady plateau is reached (red). **D** Time course recording of 22 day post-differentiation hiPSC-CM showing TRPM7 whole-cell current run-up and transient inhibition of 10mM Mg^{2+} at +80mV (red) and -80mV (black). **E** Paired individual cell current measurements at +80mV peak during extracellular solution perfusion, cells were then treated with 10mm Mg^{2+} over several minutes until current plateaued. **F** Inward current recorded at -80mV in the same cells analysed in D, after current stabilisation and after 10mM Mg^{2+} treatment. * = P<0.05, *** = P<0.001.

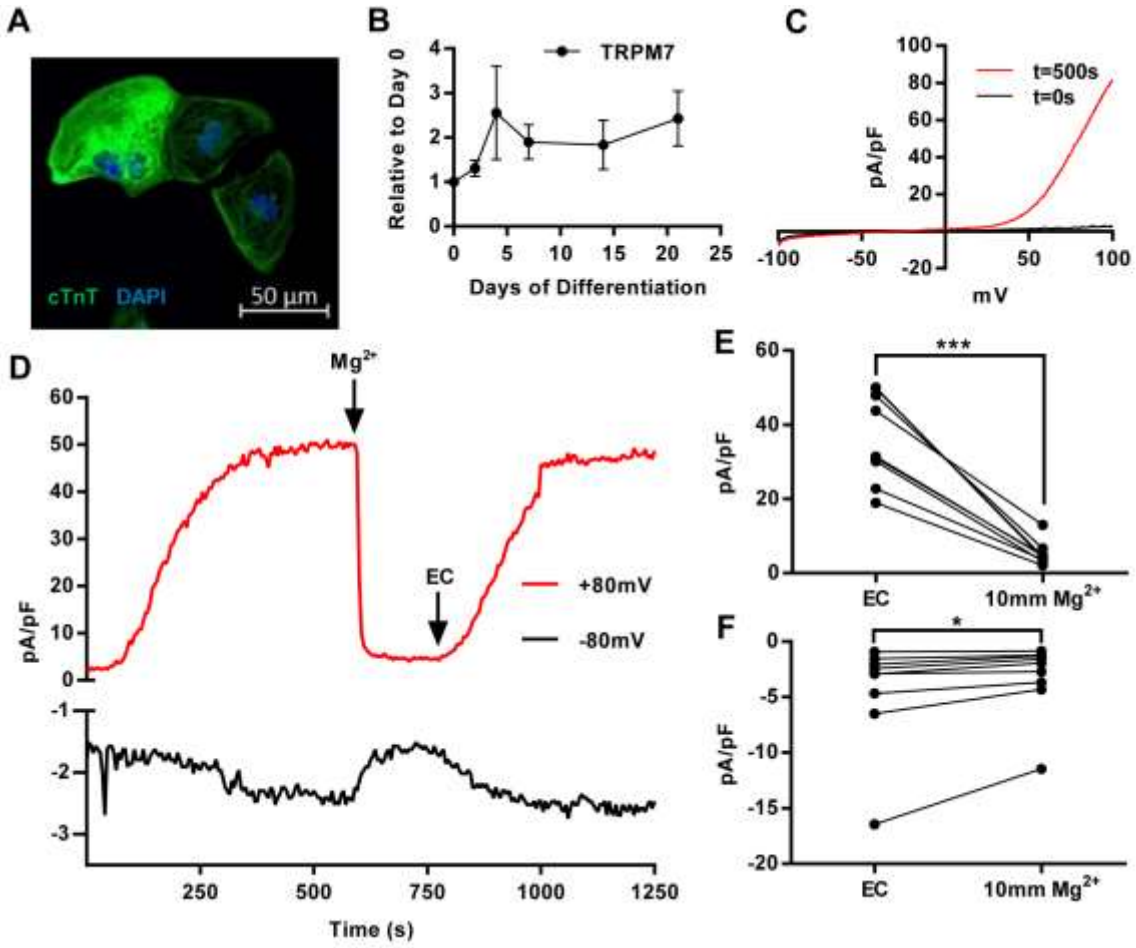

Figure 6 **siRNA mediated knockdown of TRPM7 at day 16 of differentiation does not alter hiPSC-CM AP parameters. A** Comparison of representative TRPM7 currents after run-up in hiPSC-CMs with (black) or without TRPM7 siRNA transfection (red). **B** TRPM7 current measured at +80mV following current run-up in non-targeting siRNA treated hiPSC-CMs and the effect of magnesium addition or transfection with TRPM7 siRNA. **C** Inward -80mV current measured from the same cells as in B. **D** Representative action potential trace of non-targeting siRNA treated hiPSC-CMs. **E** Representative action potential trace of hiPSC-CM transfected with siRNA-TRPM7. **F** Representative action potential trace of hiPSC-CM transfected with siRNA-scrb. **G** Maximal diastolic potential. **H** Resting membrane potential. **I** Peak voltage following action potential triggering. **J** Time to return to RMP or full **a**ction potential duration in hiPSC CMs. **K** and **L**, APD50 and APD90 measurements from the same cells in J. All recordings were done in 20-23 day old hiPSC-CMs at room temperature. Scrb = Scrambled. *** = P<0.001 vs Control.

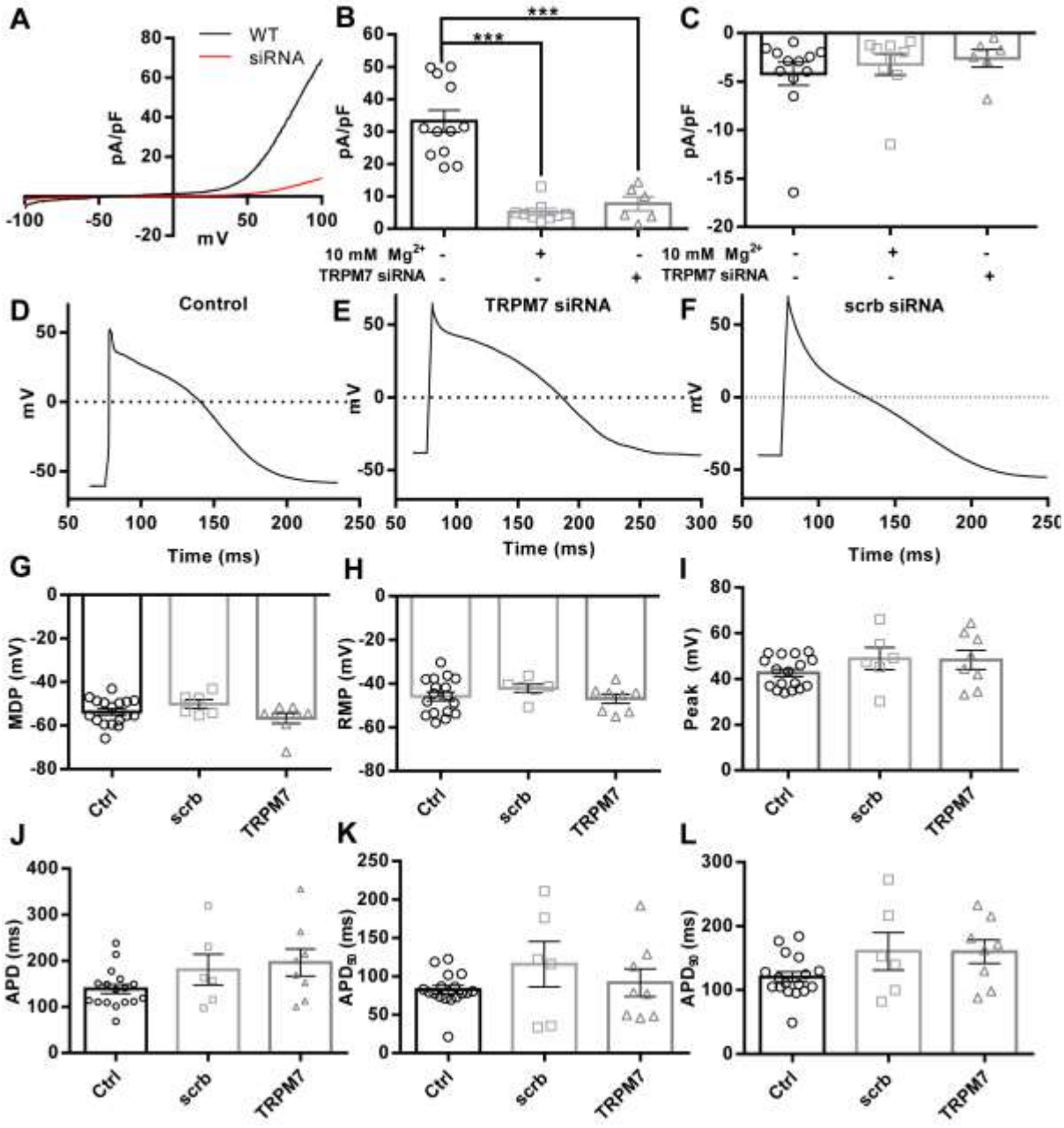

References

1 Norris, T., Manktelow, B.N., Smith, L.K. and Draper, E.S. (2017) Causes and temporal changes in nationally collected stillbirth audit data in high-resource settings. *Semin. Fetal. Neonatal. Med.*, **22**, 118-128.

2 Horn, L.C., Langner, A., Stiehl, P., Wittekind, C. and Faber, R. (2004) Identification of the causes of intrauterine death during 310 consecutive autopsies. *Eur. J. Obstet. Gynecol. Reprod. Biol.*, **113**, 134-138.

3 Bukowski, R., Carpenter, M., Conway, D., Coustan, D., Dudley, D.J., Goldenberg, R.L., Hogue, C.J.R., Koch, M.A., Parker, C.B., Pinar, H. *et al.* (2012) Causes of Death Among Stillbirths. *Obstet. Gynecol. Surv.*, **67**, 223-225.

4 Corrado, D., Basso, C. and Thiene, G. (2001) Sudden cardiac death in young people with apparently normal heart. *Cardiovasc. Res.*, **50**, 399-408.

5 Munroe, P.B., Addison, S., Abrams, D.J., Sebire, N.J., Cartwright, J., Donaldson, I., Cohen, M.M., Mein, C., Tinker, A., Harmer, S.C. *et al.* (2018) Postmortem Genetic Testing for Cardiac Ion Channelopathies in Stillbirths. *Circ. Genom. Precis Med.*, **11**, e001817.

6 Zaritsky, J.J., Redell, J.B., Tempel, B.L. and Schwarz, T.L. (2001) The consequences of disrupting cardiac inwardly rectifying K+ current (IK1) as revealed by the targeted deletion of the murine Kir2. 1 and Kir2. 2 genes. *J. Physiol.*, **533**, 697-710.

7 Arking, D.E., Pulit, S.L., Crotti, L., van der Harst, P., Munroe, P.B., Koopmann, T.T., Sotoodehnia, N., Rossin, E.J., Morley, M., Wang, X. *et al.* (2014) Genetic association study of QT interval highlights role for calcium signaling pathways in myocardial repolarization. *Nat. Genet.*, **46**, 826-836.

8 Runnels, L.W., Yue, L. and Clapham, D.E. (2001) TRP-PLIK, a bifunctional protein with kinase and ion channel activities. *Science*, **291**, 1043-1047.

9 Monteilh-Zoller, M.K., Hermosura, M.C., Nadler, M.J., Scharenberg, A.M., Penner, R. and Fleig, A. (2003) TRPM7 provides an ion channel mechanism for cellular entry of trace metal ions. *J. Gen. Physiol.*, **121**, 49-60.

10 Abiria, S.A., Krapivinsky, G., Sah, R., Santa-Cruz, A.G., Chaudhuri, D., Zhang, J., Adstamongkonkul, P., DeCaen, P.G. and Clapham, D.E. (2017) TRPM7 senses oxidative stress to release Zn(2+) from unique intracellular vesicles. *Proc. Natl. Acad. Sci.*, **114**, E6079-E6088.

11 Perraud, A.L., Zhao, X., Ryazanov, A.G. and Schmitz, C. (2011) The channel-kinase TRPM7 regulates phosphorylation of the translational factor eEF2 via eEF2-k. *Cell Signal*, **23**, 586-593.

12 Krapivinsky, G., Krapivinsky, L., Manasian, Y. and Clapham, D.E. (2014) The TRPM7 Chanzyme Is Cleaved to Release a Chromatin-Modifying Kinase. *Cell*, **157**, 1061-1072.

13 Desai, B.N., Krapivinsky, G., Navarro, B., Krapivinsky, L., Carter, B.C., Febvay, S., Delling, M., Penumaka, A., Ramsey, I.S., Manasian, Y. *et al.* (2012) Cleavage of TRPM7 releases the kinase domain from the ion channel and regulates its participation in Fas-induced apoptosis. *Dev. Cell*, **22**, 1149-1162.

14 Schilling, T., Miralles, F. and Eder, C. (2014) TRPM7 regulates proliferation and polarisation of macrophages. *J. Cell. Sci.*, **127**, 4561-4566.

15 Sah, R., Mesirca, P., Mason, X., Gibson, W., Bates-Withers, C., Van den Boogert, M., Chaudhuri, D., Pu, W.T., Mangoni, M.E. and Clapham, D.E. (2013) Timing of myocardial trpm7 deletion during cardiogenesis variably disrupts adult ventricular function, conduction, and repolarization. *Circulation*, **128**, 101-114.

16 Sah, R., Mesirca, P., Van den Boogert, M., Rosen, J., Mably, J., Mangoni, M.E. and Clapham, D.E. (2013) Ion channel-kinase TRPM7 is required for maintaining cardiac automaticity. *Proc. Natl. Acad. Sci.*, **110**, E3037-E3046.

17 Hermosura, M.C., Nayakanti, H., Dorovkov, M.V., Calderon, F.R., Ryazanov, A.G., Haymer, D.S. and Garruto, R.M. (2005) A TRPM7 variant shows altered sensitivity to magnesium that may contribute to the pathogenesis of two Guamanian neurodegenerative disorders. *Proc. Natl. Acad. Sci.*, **102**, 11510-11515.

18 Ng, P.C. and Henikoff, S. (2003) SIFT: predicting amino acid changes that affect protein function. *Nucleic Acids Res*, **31**, 3812-3814.
19 Adzhubei, I., Jordan, D.M. and Sunyaev, S.R. (2013) Predicting functional effect of human missense mutations using PolyPhen-2. *Curr. Protoc. Hum. Genet.*, **76**, 7-20.
20 Burridge, P.W., Matsa, E., Shukla, P., Lin, Z.C., Churko, J.M., Ebert, A.D., Lan, F., Diecke, S., Huber, B., Mordwinkin, N.M. *et al.* (2014) Chemically defined generation of human cardiomyocytes. *Nat. Methods*, **11**, 855-860.
21 Schwartz, P.J., Stramba-Badiale, M., Segantini, A., Austoni, P., Bosi, G., Giorgetti, R., Grancini, F., Marni, E.D., Perticone, F., Rosti, D. *et al.* (1998) Prolongation of the QT interval and the sudden infant death syndrome. *New Eng. J. Med.*, **338**, 1709-1714.
22 Ryazanova, L.V., Rondon, L.J., Zierler, S., Hu, Z.X., Galli, J., Yamaguchi, T.P., Mazur, A., Fleig, A. and Ryazanov, A.G. (2010) TRPM7 is essential for Mg2+ homeostasis in mammals. *Nat. Commun.*, **1**, 109.
23 Duan, J., Li, Z., Li, J., Hulse, R.E., Santa-Cruz, A., Valinsky, W.C., Abiria, S.A., Krapivinsky, G., Zhang, J. and Clapham, D.E. (2018) Structure of the mammalian TRPM7, a magnesium channel required during embryonic development. *Proc. Natl. Acad. Sci.*, **115**, E8201-E8210.
24 Du, J., Xie, J., Zhang, Z., Tsujikawa, H., Fusco, D., Silverman, D., Liang, B. and Yue, L. (2010) TRPM7-mediated Ca2+ signals confer fibrogenesis in human atrial fibrillation. *Circ. Res.*, **106**, 992-1003.
25 Hedley, P.L., Jorgensen, P., Schlamowitz, S., Wangari, R., Moolman-Smook, J., Brink, P.A., Kanters, J.K., Corfield, V.A. and Christiansen, M. (2009) The genetic basis of long QT and short QT syndromes: a mutation update. *Hum. Mutat.*, **30**, 1486-1511.
26 Crotti, L., Tester, D.J., White, W.M., Bartos, D.C., Insolia, R., Besana, A., Kunic, J.D., Will, M.L., Velasco, E.J., Bair, J.J. *et al.* (2013) Long QT syndrome-associated mutations in intrauterine fetal death. *JAMA*, **309**, 1473-1482.
27 Miller, D.C., Harmer, S.C., Poliandri, A., Nobles, M., Edwards, E.C., Ware, J.S., Sharp, T.V., McKay, T.R., Dunkel, L., Lambiase, P.D. *et al.* (2017) Ajmaline blocks INa and IKr without eliciting differences between Brugada syndrome patient and control human pluripotent stem cell-derived cardiac clusters. *Stem. Cell. Res.*, **25**, 233-244.
28 Davydov, E.V., Goode, D.L., Sirota, M., Cooper, G.M., Sidow, A. and Batzoglou, S. (2010) Identifying a High Fraction of the Human Genome to be under Selective Constraint Using GERP plus. *Plos Comput Biol*, **6**, e1001025.